JOURNAL OF THEORETICAL
AND APPLIED MECHANICS
3, **37**, 1999

NUMERICAL SIMULATION OF BONE-IMPLANT SYSTEMS USING A MORE REALISTIC MODEL OF THE CONTACT INTERFACES WITH ADHESION

JERZY ROJEK

JÓZEF JOACHIM TELEGA

Institute of Fundamental Technological Research, Warsaw
e-mail: jtelega@ippt.gov.pl

The aim of the paper is twofold. First, most important notions concerning adhesion are discussed. Modelling of unilateral contact with adhesion between two deformable bodies is studied. The initial boundary value problem for contact with adhesion is discussed, including its regularization. Second, numerical analysis of the behaviour of the femur with implant is studied under quasi-static loading.

Key words: joint replacement, FEM, interface, contact, adhesion

1. Introduction

The finite element method applied to the total hip replacement is usually used to study the load transfer between the components of the bone-implant system: stem, cement and bone and the resulting stress distribution in these components. The load transfer mechanism and the associated stress patterns in prosthetic fixation depend on four aspects: loading characteristics, geometry, material properties and boundary/interface conditions. It was shown by Weinans et al. (1990) that of these four the interface conditions represent by far the most important aspect. At the same time the bone-cement and cement-stem interfaces in the cemented implants as well as the bone-stem interface in the cementless implant are very complicated structures for finite element modelling. Usually quite simple assumptions have been made in the modelling of these interfaces.

The aim of the present paper is twofold. First, we shall discuss most important notions concerning adhesion. Phenomenological approach to modelling of

adhesion is also examined. Secondly, the finite element model of the hip implant system with a more realistic model of contact interfaces taking into account the adhesive forces will be formulated.

Total hip replacement (THR) has become one of the major surgical advances of this century. An estimated number of operations is between 500 000 and 1 million per year, cf Huiskes and Verdonschot (1997). The THR is an effective treatment for serious forms of osteoarthritis and for disabling effects of rheumatoid arthritis, congenital deformities, and particular kinds of posttraumatic conditions. According to Huiskes and Verdonschot (1997), when the cause of degenerative joint disease is mechanically initiated, as is often the case, this disease is better referred to as osteoarthritis.

The successful application of THR on a large scale, which has essentially evolved over the last three decades, is an accomplishment of scientific and technological developments in orthopaedic surgery and bioengineering. Of particular importance has been the impact coming from biomaterials and biomechanics sciences. The proliferation of applications started around 1960 with the introduction of two inventions due to Sir John Charnley, cf Huiskes and Verdonschot (1997). One was the adoption of the *low-friction* principle, whereby a relatively small metal femoral head was made to rotate against a polyethylene acetabular cup. Another was the use of acrylic cement (polymethylmethacrylate or PMMA) as a filling material to accomodate uniform load transfer between the smooth-shaped prosthesis and the irregular texture of the bone. The PMMA forms a solid but relatively flexible mantle between bone and prosthesis. It is a relatively weak material, however, and long-term loosening of prostheses has been attributed to its mechanical desintegration.

The efforts to improve the endurance of implant fixation have resulted in better cementing techniques. Alternative prosthetic designs aimed at replacing acrylic cement with other means of fixation. Early cementless prostheses were the press-fitted or screwed-in types. Cementless porous-coated prostheses were introduced to provoke bone ingrowth for improved fixation. Hydroxyapatite-coated hip prostheses are meant to form a firm biological adhesive bond with bone (osseous integration). Some of the cementless devices have failed, but other behave well in the mid- to long-term. Definite conclusions about their ultimate clinical performances and about the best fixation methods or designs require longer-term studies. We observe that the cementless prostheses are used predominantly in younger patients (< 60 years), where it is assumed that these prostheses eventually simplify a revision operation.

Before the late 1960s, the treatment for knee arthritis were osteotomy, debridement, synovectomy, interposing of metallic femoral condyles or tibial

blocks, and cementless metal hinges. In 1969, a cemented metal-plastic condylar replacement, the *polycentric*, was developed by Gunston, cf Walker and Blunn (1997). This design, using the same cemented metal-plastic technology as devised for the hip by Charnley, was the forerunner of the modern-day condylar replacement. Since that time, the term *total knee replacement* (TKR) has taken on a broad meaning encompassing the replacement of femoral, tibial and patellofemoral bearing surfaces and including the complete mechanical replacement of the joint surfaces and ligaments with fixed and rotated hinges. Since 1969, TKR development has been an evolutionary process, relying on intuitive design, empirical data, and laboratory studies. As a result, the clinical outcomes of different designs have varied considerably. Paradoxically, some of the design introduced in the 1970s had successful long-term results, whereas some introduced more recently have exhibited serious problems. Although the design goals themselves might be well recognized, data on the mechanical conditions under which the TKRs operate are far from complete. To date, the materials for TKR have been predominantly cobalt-chrome articulating on ultra-high molecular weight polyethylene (UHMPWE). Titanium alloy has been used but is not preferred because of its susceptibility to three-body abrasive wear, cf Telega et al. (1999). Ceramic, or metal with a ceramic coating has been used for the femoral component, and in some designs even ceramic-on-ceramic are used, where the rationale is the reduction of friction and wear. For interfacing the components to the bone, acrylic cement continues to be the most popular method, though porous coatings of various types or macrotextures with hydroxyapatite coating are also being used.

All in all, it is our strong conviction that adhesion at interfaces plays an important role in successful functioning of hip and knee prostheses, cf Fig.1.

2. Fixation of the stem in the total hip replacement

Fixation of a prosthesis in a femur in the total hip replacemnt is one of the most important mechanical aspects of the performance of the bone-implant system. Femoral component loosening is a main failure in this type of treatment (Huiskes, 1979). The loosening is usually accompanied by a pain and most often it requires a reoperation. Durability of the fixation is the factor deciding about a long-term success of the operation.

Loosening can be caused by a variety of mechanical and biological phenomena. It is widely accepted that loosening of a cemented stem is usually

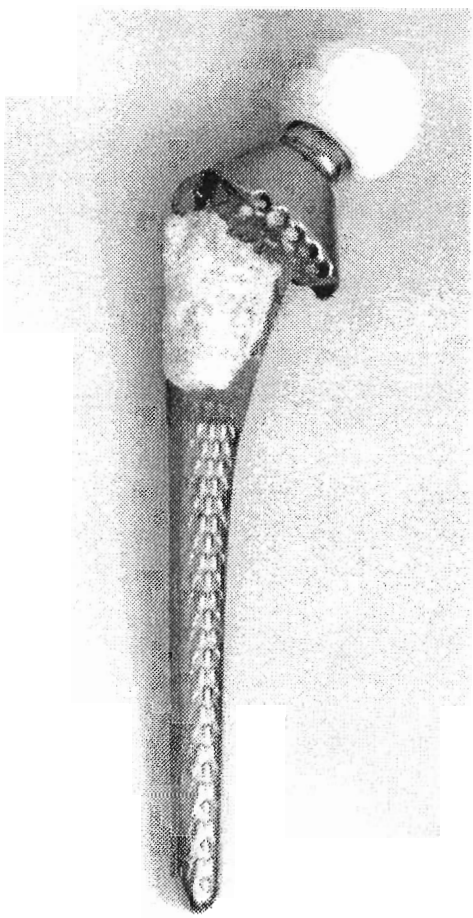

Fig. 1. Removed stem with clearly visible zone of strong adhesion

initiated by debonding at the stem-cement interfaces. Adhesion between the stem and bone is decisive for the fixation of the cementless implants.

The numerical analysis can allow better comprehension of the mechanical behaviour of the hip-prosthesis system leading to better design and longer durability of the prosthesis. The numerical model, however, should take into account complex behaviour at the interfaces of the hip-implant system.

In the present paper our considerations are focussed on the bone-cement-femoral stem system. We observe, however, that a good long-term fixation of the acetabular socket remains a difficult problem, particularly in the case of cemented arthroplasty revision, cf Raut et al. (1997).

3. Bone-cement interface

The cement-bone interface is a key region for success of the joint replacement (Huiskes, 1979). Fixation of acrylic cement to cancellous surfaces is achieved by means of two mechanisms: (1) by conforming and anchoring to the gross configurations and irregularities produced on the surface by the surgeon, and (2) by penetration of the cement into the microstructure of the cancellous surface. There is no chemical bond between the acrylic cement and the bone.

The mechanical strength of the cement-cancellous bone interlock depends on the preparation of bone surface and the technique used to apply the cement. The finger-packing of the cement, used in early operations, resulted in low penetration of the cement and lower strength of the interface. Pressurization of the cement into the bone provided significant strength improvements (Krause et al., 1981) due to increased penetration into the cancellous bone and formation of a cement-bone composite.

The experimental tensile and shear tests (Krause et al., 1981) show that for the bone-cement interfaces obtained with pressure injection of the cement the tensile strength is about 8 ± 3 MPa and the shear strength 25 ± 7 MPa. Slightly higher values are obtained if the bone surface is specially cleaned.

The strength of the bone-cement interface is affected by biological changes in the region of interface (Huiskes, 1979). In the first postoperative period a layer of necrotic bone a few mm thick is observed at the interface, it is believed that the principal causes of this phenomenon can be reaming of the implant bed and disturbed vascularity. Later, postoperatively, the layer of necrotic bone is resorbed and replaced by a soft tissue in which new bone is formed. In this process a good mechanical interlocking can be lost. A new bone may be separated from the direct contact with the cement by a fibrous tissue layer, if this layer is abnormally thick, it usually signifies a forthcoming loosening. Some authors believe that occurence of this layer is related to micromovents and stresses at the interface (Willert et al., 1974; Rubin et al., 1992).

4. Metal-cement interface

The bond between cement and metal is quite weak – much weaker than the strength of the bulk cement. There was, however, a controversy if it was desirable to have a strong bonding between the metal and cement. It has been

postulated that it is essential to have the cement-metal interface slip to protect the cement-bone interface. The clinical studies argue against this hypothesis (Harris, 1992).

Debonding of the cement-metal interface is the dominant mode by which loosening is initiated. Because of high strains at the tip of the prosthesis during stair climbing and gait, debonding often starts at or near the tip. Because of high torsional loads in stair climbing and rising from a chair debonding also frequently begins proximally.

Porous coating of the stem strengthens the metal-cement interface, the tensile strength of this interface is about 20% of the strength of the cement itself (Raab et al., 1981).

5. Bone-metal interface in cementless total hip replacement

Adhesion should be considered in cementless total hip replacement as well. After cementless total hip replacement, bone ingrowth takes place between the bone and the prosthesis. This ingrowth is considered to be of fibre-type. It is known that a bone fibre exerts some adhesive force and plays an important role in the biological fixation after cementless total hip replacement. A porous coated prosthetic stem is thought to allow for a better ingrowth and a better three dimensional interlock between the implant and bone. After ingrowth the porous coated fixation can transfer tensile stress across the interface between bone and implant.

This is in contrast to a smooth metal stem which cannot transfer tensile stresses and can only transfer shear stresses across the regions where compressive normal contact stresses at the interface exist.

In some modern designs, prosthetic stems are only proximally porous coated while in to other the coating is limited to some regions. Partially coated stems are thought to provide reduced areas for corrosion, easier removal of an infected or loose implant, and increased implant fatigue life (Bobyn et al., 1985).

6. Interfaces in finite element modelling

The finite element method has been used for many years for the analysis of bone-prosthesis structures. Most of the work were done for the hip joint,

although a number of studies of other joints can be found in the relevant literature – the review of recent finite element applications in orthopaedic mechanics can be found in Mackerle (1998). Most of the investigations aimed at predicted of stress levels and stress distribution in a bone and prosthesis. The finite element method has been applied to optimization of the prosthesis design as well as to study failure modes of the artificial joints.

Early studies were often made on two-dimensional models (Huiskes et al., 1982; Huiskes, 1979). Three-dimensional analysis have been started using linear finite element programs (Vichnin and Batterman, 1985), more sophisticated models have been analysed using nonlinear methods (Rohlmann et al., 1988).

Most of these models have assumed a perfect bonding with compatibility of displacements at the bone-cement and stem-cement interfaces (which is equivalent to the assumptions of infinite strength of the interface). Rigid bonds across the interface were used by Crowninshield et al. (1980), Huiskes and Chao (1983) and others.

The models with rigid bonds across the interface do not describe properly not only a mechanism of the interface but the load transfer in the bone-implant system, as well. It was shown that using non-bonded interfaces yields in substantially different stress fields (Mann et al., 1995; Rohlmann et al., 1988). The effect of bone-prosthesis bonding on load transfer in total hip replacement was investigated by McNamara et al. (1997). The contact with Coulomb friction was incorporated into the finite element model of a hip-implant system by Rubin et al. (1992) giving the possibility to evaluate the relative micromotions at the bone-implant interface. Different models of a fibrous membrane between cement and bone in a total hip replacement were investigated by Weinans et al. (1990). It was shown that the effects of a fibrous membrane cannot be described satisfactorily using simple models.

Neglecting tensile force transfer across the interface, justified in the case of fibrous membrane, is a serious drawback in modelling the interfaces with a significant adhesive force. All the models using the standard frictional formulation (Mann et al., 1995; Rohlmann et al., 1988; McNamara et al., 1997; Rubin et al., 1992; Weinans et al., 1990) not only neglect tensile stresses at the interfaces but allow the shear stresses only when the contact pressure is compressive.

Considering the adhesive forces as an important factor in modelling the interfaces of joint replacement we have developed a contact algorithm allowing for adhesive forces that will be described in the next section. This allows one to create a more realistic finite element model of a joint replacement.

7. Modelling the interface as a contact problem with adhesion

Tissue assembly development and other biological functions (like identification and removal of foreign bodies in immune defense) involve complex adhesive interactions. Biologists have identified and isolated many molecular *adhesions* responsible for cellular adhesion processes, cf Evans (1995), Evans and Ritchie (1997), Kendall et al. (1998). Cellular adhesion is out of the scope of our presentation. However, the problem whether the osteocyte adhesion at the bone-implant or bone-cement interfaces plays a significant role seems to be completely unresolved.

In the present section we first recall some fundamental notions concerning adhesion. Next, we propose a general approach to the formulation of unilateral contact problem with adhesion.

7.1. Adhesion: some basic notions

According to Kendall (1994) there is a difference between adhesion at the molecular level and adhesion in engineering. The lack of adhesion that we observe in engineering circumstances is rather an aberration that depends on the mechanisms of contact than on molecular adhesion. If we define the molecular forces through the work of adhesion per unit area of contact, equations for the mechanical force of adhesion in particular geometries are briefly examined below. Primarily, however, we observe that adhesion between two solids may be due to ionic, covalent metallic, hydrogen or van der Waals forces; for more details the reader is referred to Kendall (1994), Maugis (1982), Maugis and Barquins (1980). To cut these bonds and to reversibly separate the two solids 1 and 2 in contact on unit area, the energies γ_1 and γ_2 are needed to create the unit areas 1 and 2, whereas the excess energy γ_{12} (interfacial energy) is recovered. The quantity

$$w = \gamma_1 + \gamma_2 - \gamma_{12} \tag{7.1}$$

is the *Dupré energy of adhesion* or the *thermodynamic work of adhesion*. We observe that for a single crystal one has $\gamma_{12} = 0$; between two grains of polycrystal γ_{12} is the grain boundary energy ($\gamma_{GB} = \gamma/3$) or the twin boundary energy ($\gamma_{TB} = \gamma/50$).

The separation never occurs as a whole, but by progression of a crack. During this propagation interface bonds are broken, elastic energy is released and irreversible work is dissipated at the crack tip.

Work of adhesion is a useful quantity because it distinguishes the two states, contact and separation. This work is done over a very small distance for

van der Waals forces, 99% of the work is reached when the surfaces are pulled 1 nm apart. For other types of bonding, such as ionic and covalent, even smaller distances are involved. Thus, the precise shape of the force separation curve need not to be known to understand many phenomena. Indeed, the precise shape may even not be measurable because of the instability of spontaneous jumping of smooth surfaces into contact.

Kendall (1994) summarized the available formulae for the mechanical force F needed to separate two contacting bodies depicted in Fig.2.

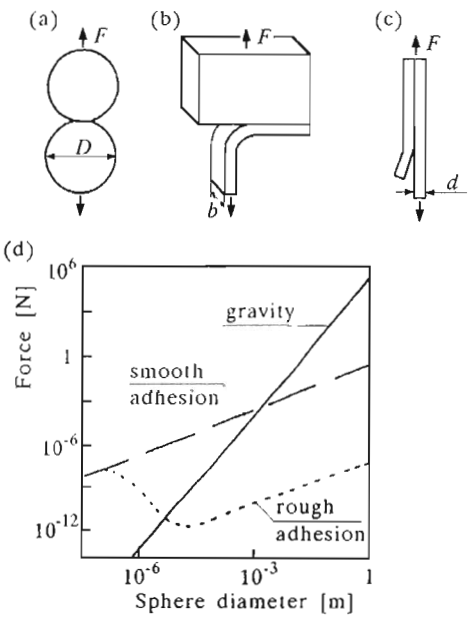

Fig. 2. (a) Two identical spheres in contact under the van der Waals attraction with a force F applied to separate them; (b) peeling of an elastic film from a rigid surface; (c) cracking of a lap joint; (d) comparison of the adhesion force with gravity force for very smooth and rough spheres of different diameteres, after Kendall (1994)

The force F needed to separate from molecular contact two identical spherical particles of diameter D and the work of adhesion w (Fig.2a) is given by

$$F = kwD \tag{7.2}$$

where k is a constant near unity. For elastic spheres $k = 3\pi/8$.

A polymer film peeling from a rigid substrate is also described by Eq (7.2), but with D replaced by the film width (Fig.2b).

In more complex situations, where the joint is stretched significantly during

breakage as in the lap joint (Fig.2c), the elastic modulus E and thickness d of the materials become important and the adhesion criteria for fracture becomes

$$F = b\sqrt{4wEd} \tag{7.3}$$

which has the same form as Griffith's cracking equation for glass.

These equations are instructive because they show that adhesion force can vary substantially with geometry and material stiffness, as well with the molecular surface quantitied by w.

Kendall (1994) discussed also the influence of fluid molecules on contacting solid surfaces. Other interacting adhesion mechanisms are adhesive drag, hysteresis, stringing and clustering.

7.2. Modelling of unilateral contact with adhesion

Fremond (1987a), (1988) developed a general framework for the study of contact problems with adhesion. The main idea consists in introducing the *intensity of adhesion* $\beta(\boldsymbol{x}, t)$ where $\boldsymbol{x} \in \Gamma_c$ and t stands for the time variable. Here Γ_c is the surface of potential contact. To simplify the presentation, let us first consider the unilateral contact with adhesion of a deformable body, occupying a domain Ω of $\mathbb{R}^3$ in its undeformed configuration, with a rigid obstacle. Contact of deformable bodies simulating the bone-prosthesis or bone-cement-prosthesis system will also be considered.

The intensity of adhesion β is such that:

- $\beta = 1$ all the bonds are active,
- $\beta = 0$ all the bonds are broken or the adhesion is absent,
- $0 < \beta < 1$, a part β of the the bonds remain active, the remaining bonds are broken, the adhesion is partial.

Let $\Gamma = \partial\Omega$ consists of three parts: Γ_0, Γ_1 and Γ_c such that $\Gamma = \overline{\Gamma}_0 \cup \overline{\Gamma}_1 \cup \overline{\Gamma}_c$. Here the bar denotes the closure of set. Consider a linear elastic body satisfying

$$\begin{aligned} &\sigma_{ij,j} + f_i = 0 && \text{in } \Omega \\ &\boldsymbol{u} = \boldsymbol{0} && \text{on } \Gamma_0 \\ &\sigma_{ij} n_j = g_i && \text{on } \Gamma_1 \\ &\sigma_{ij} n_j = R_i && \text{on } \Gamma_c \end{aligned} \tag{7.4}$$

and

$$\sigma_{ij} = a_{ijkl} e_{ij}(\boldsymbol{u}) \tag{7.5}$$

where

$$e_{ij}(\boldsymbol{u}) = u_{(i,j)} = \frac{1}{2}\Big(\frac{\partial u_i}{\partial x_j} + \frac{\partial u_j}{\partial x_i}\Big)$$

The elastic moduli a_{ijkl} are functions of $L^\infty(\Omega)$ and satisfy the following condition

$$\exists c_1 \geqslant c_0 > 0 \quad \forall \boldsymbol{\epsilon} \in I\!E_s^3 \qquad c_0 \epsilon_{ij}\epsilon_{ij} \leqslant a_{ijkl}(\boldsymbol{x})\epsilon_{ij}\epsilon_{kl} \leqslant c_1 \epsilon_{ij}\epsilon_{ij} \tag{7.6}$$

for almost every $\boldsymbol{x} \in \Omega$. Here $I\!E_s^3$ stands for the space of symmetric 3×3 matrices, whilst $\boldsymbol{n} = (n_i)$ denotes the outward unit normal to Γ. Obviously, the functions $\boldsymbol{g}$ and $\boldsymbol{f}$ are prescribed. Our assumptions allow the body to be made of anisotropic material. Let $\boldsymbol{w} = (w_i)$ denote displacement field of the rigid foundation. We set

$$[\![\boldsymbol{u}]\!] = \boldsymbol{u} - \boldsymbol{w} \tag{7.7}$$

The jump $[\![\boldsymbol{u}]\!]$ and the adhesion intensity β are not independent since they satisfy

$$0 \leqslant \beta \leqslant 1 \qquad \beta[\![\boldsymbol{u}]\!] = \boldsymbol{0} \qquad [\![\boldsymbol{u}]\!] \cdot \boldsymbol{n} \leqslant 0 \quad \text{on } \Gamma_c \tag{7.8}$$

The condition (7.8) implies that for $[\![\boldsymbol{u}]\!] \neq \boldsymbol{0}$ there is no interaction between the structure and the foundation, i.e., $\beta = 0$.

It is natural to introduce the following *nonconvex* set of constraints

$$K = \{(\gamma, \boldsymbol{v}) | 0 \leqslant \gamma \leqslant 1\,, \ \gamma \boldsymbol{v} = \boldsymbol{0}\,, \ \boldsymbol{v} \cdot \boldsymbol{n} \leqslant 0 \ \text{ on } \Gamma_c\} \tag{7.9}$$

From now on we set $\boldsymbol{w} = \boldsymbol{0}$. By I_K we denote the indicator function of the set K, cf Rockfellar and Wets (1998)

$$I_K(\gamma, \boldsymbol{v}) = \begin{cases} 0 & \text{if } (\gamma, \boldsymbol{v}) \in K \\ +\infty & \text{otherwise} \end{cases} \tag{7.10}$$

Many possibilities are offered to model the contact with adhesion between Ω and the foundation. Consider now some physically motivated cases:

(i) The adhesion is described by using the generalized potential $\varphi(\beta, \boldsymbol{u})$; for instance

$$\varphi(\beta, \boldsymbol{u}) = \int_{\Gamma_c} \Big(\frac{k}{2}|\boldsymbol{u}|^2 - w\beta\Big)\, d\Gamma + I_K(\beta, \boldsymbol{u}) \tag{7.11}$$

where k is a non-negative constant and w stands for the Dupré energy, introduced earlier.

In general, adhesion action on Γ_c consists of the interior force F with the dimension of a surface work and the external force A. For instance, A may be the electrostatic force modifying the contact. In the case of the contact bone-prosthesis A may model the forces existing in a thin membrane, which develops between the bone and the prosthesis, cf Ingham and Fischer (1999).

Anyway, we have

$$F = A \tag{7.12}$$

In many practical situations A disappears. It is natural to split F into the reversible F^e and irreversible parts F^i (on Γ_c). We have

$$(F^e, \boldsymbol{R}) \in \partial\varphi(\beta, \boldsymbol{u}) \tag{7.13}$$

where $\partial\varphi$ denotes the *local subdifferential* of the the potential φ, cf Fremond (1987a), (1988). We observe that I_K is not a convex function. Consequently, in the constitutive relationship (7.13) $\partial\varphi$ cannot be the usual subdifferential, cf Rockfellar and Wets (1998). Alternatively, $\partial\varphi$ can be interpreted as Clarke's subdifferential, cf Rockfellar and Wets (1998). The last notion was not employed by Fremond (1987a), (1988).

To describe the irreversible part F^i of F, we introduce a convex, positive functional Φ of $\dot{\beta} = d\beta/dt$, such that $\Phi(0) = 0$. Then

$$F^i \in \partial\Phi(\dot{\beta}) \tag{7.14}$$

where $\partial\Phi$ denotes the subdifferential of Φ. We recall that

$$\partial\Phi(\dot{\beta}) = \Big\{G | \Phi(\gamma) - \Phi(\dot{\beta}) \geqslant \int_{\Gamma_c} G(\gamma - \dot{\beta})\, d\Gamma \quad \forall\gamma\Big\} \tag{7.15}$$

For instance, a nonlinear viscous potential of the Norton-Hoff type is given by

$$\Phi(\dot{\beta}) = \int_{\Gamma_c} \frac{1}{p}\Big[(\omega * \dot{\beta})\dot{\beta}\Big]^{\frac{p}{2}}\, d\Gamma = \frac{1}{p}\Big(\langle \omega * \dot{\beta}, \dot{\beta}\rangle\Big)^{\frac{p}{2}} \tag{7.16}$$

Here $*$ denotes the convolution product and ω is a C^∞-function, which is positive, and $p > 1$. For $p = 2$ we have

$$\begin{aligned} \Phi(\dot{\beta}) &= \frac{1}{2}\langle \omega * \dot{\beta}, \dot{\beta}\rangle = \frac{1}{2}\int_{\Gamma_c} (\omega * \dot{\beta})\dot{\beta}\, d\Gamma \\ F^i &= \omega * \dot{\beta} = \int_{\Gamma_c} \omega(\boldsymbol{x} - \boldsymbol{y})\dot{\beta}(\boldsymbol{y})\, dy \end{aligned} \tag{7.17}$$

Introducing the energy release rate denoted by H (cf Fremond, 1987a,b), (1988), one can consider all possible situations occurring during the contact, i.e., the total adhesion ($\boldsymbol{u} = \boldsymbol{0}$, $\beta = 1$, on Γ_c), partial adhesion ($\boldsymbol{u} = \boldsymbol{0}$, $0 < \beta < 1$), contact without adhesion ($\boldsymbol{u} = \boldsymbol{0}$, $\beta = 0$), and lack of adhesion ($\boldsymbol{u} \neq \boldsymbol{0}$, $\beta = 0$).

We omit the details. It is worth noting, however, that for $\boldsymbol{u} \neq \boldsymbol{0}$ and $\beta = 0$ we have

$$R_n + ku_n \leqslant 0 \qquad (R_n + ku_n)u_n = 0 \qquad \boldsymbol{R}_T + k\boldsymbol{u}_T = \boldsymbol{0} \quad \text{on } \Gamma_c \tag{7.18}$$

where $R_n = R_i n_i$, $u_n = u_i n_i$, $\boldsymbol{R}_T = \boldsymbol{R} - R_n\boldsymbol{n}$, $\boldsymbol{u}_T = \boldsymbol{u} - u_n\boldsymbol{n}$. If F^i is given by Eq (7.17)$_2$, then $F^i(\boldsymbol{x})$ does not necessarily vanishes even for $\boldsymbol{x}$ belonging to the decohesion zone.

(ii) Consider now the contact with adhesion and friction. The potential (7.11) is replaced by

$$\varphi_1(\beta, \boldsymbol{u}, \dot{\boldsymbol{u}}_T) = \int_{\Gamma_c} \left(\frac{k}{2}u_n^2 - w\beta\right) d\Gamma + \int_{\Gamma_c} D(\boldsymbol{R}_n, -\dot{\boldsymbol{u}}_T)\, d\Gamma + I_K(\beta, \boldsymbol{u}) \tag{7.19}$$

Here D denotes the friction dissipation density, cf Telega (1988). It may be assumed that D depends additionally on β. The function $D(R_n, \cdot)$ is assumed to be convex, thus D is subdifferentiable with respect to the second argument. We recall that $D(R_n, \cdot)$ is finite and lower semi-contionuous. The reaction $\boldsymbol{R}$ is written as follows

$$\boldsymbol{R} = \boldsymbol{R}_n + \boldsymbol{R}_T = R_n\boldsymbol{n} + \boldsymbol{R}_T$$

Instead of Eq (7.13) we have

$$(F^e, \boldsymbol{R}_n, \boldsymbol{R}_T) \in \partial\varphi_1(\beta, \boldsymbol{u}, \dot{\boldsymbol{u}}_T) \tag{7.20}$$

Now the condition (7.18)$_3$ is to be replaced by

$$\boldsymbol{R}_T \in \partial_2 D(\boldsymbol{R}_n, -\dot{\boldsymbol{u}}_T) \tag{7.21}$$

and expresses the friction law. Here $\partial_2 D(\boldsymbol{R}_n, -\dot{\boldsymbol{u}}_T)$ stands for the partial subdifferential with respect to the second argument. In the case of the Coulomb friction we have

$$\boldsymbol{R}_T = -\lambda\dot{\boldsymbol{u}}_T \qquad \lambda \geqslant 0 \tag{7.22}$$

(iii) Consider now the viscous behaviour with impossible bond restitution. Let $\mathcal{M}^-(\Gamma_c)$ be the set of negative measures on Γ_c. The function β can be

discontinuous. The space of functions with bounded variation constitutes a proper mathematical framework for β, cf Moreau (1988), Telega and Gałka (1998). We introduce the following potential for F^i

$$\Phi_1(\dot{\beta}) = \frac{1}{2}\langle \omega * \dot{\beta}, \dot{\beta} \rangle + I_{\mathcal{M}^-}(\dot{\beta}) \tag{7.23}$$

where

$$I_{\mathcal{M}^-}(\dot{\beta}) = \begin{cases} 0 & \text{if } \dot{\beta} \in \mathcal{M}^- \\ +\infty & \text{otherwise} \end{cases} \tag{7.24}$$

Denote by $\mathcal{O}$ the interior of the support of $\dot{\beta}$, then

$$\begin{aligned} F^i(\boldsymbol{x}) &= (\omega * \dot{\beta})(\boldsymbol{x}) \qquad \text{if } \boldsymbol{x} \in \mathcal{O} \\ F^i(\boldsymbol{x}) &\geqslant (\omega * \dot{\beta})(\boldsymbol{x}) \qquad \text{if } \boldsymbol{x} \notin \mathcal{O} \end{aligned} \tag{7.25}$$

Also in this case one can consider the unilateral frictionless contact or unilateral contact with friction. In the former case φ is given by Eq (7.11) whilst in the latter case the constitutive modelling involves φ_1 given by Eq (7.13).

(iv) One can envisage much more complicated contact modelling involving adhesion and friction. For instance, it is possible to develop a first gradient theory involving $\nabla\beta$, cf Fremond (1987b). The reversible part F^e of F may be modelled by a non-quadratic, or even non-convex expression instead of $k|\boldsymbol{u}|^2/2$. The coated parts of cementless prostheses can be modelled by using fractals. It would also be interesting and very useful to include the influence of wear debris on loss of adhesion, cf Telega et al. (1999).

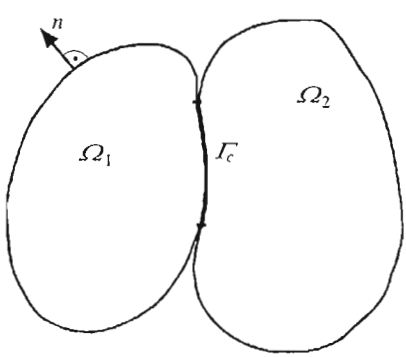

Fig. 3. Two deformable bodies in contact

(v) Consider now the contact of two deformable bodies, cf Fig.3. Γ_c is now the surface of potential contact. Now $[\![\boldsymbol{u}]\!] = \boldsymbol{u}^{(1)} - \boldsymbol{u}^{(2)}$, $\boldsymbol{R} = \boldsymbol{R}^{(1)} = -\boldsymbol{R}^{(2)}$. The unit normal vector $\boldsymbol{n}$ is taken as exterior to $\partial\Omega_1$.

The set K of constraints is to be replaced by

$$K_1 = \left\{(\gamma, [\![\boldsymbol{u}]\!]),\ [\![\boldsymbol{u}]\!] = \boldsymbol{u}^{(1)} - \boldsymbol{u}^{(2)} | 0 \leqslant \gamma \leqslant 1,\ \gamma[\![\boldsymbol{u}]\!] = \boldsymbol{0}\,,\ [\![\boldsymbol{u}]\!] \leqslant 0 \text{ on } \Gamma_c\right\} \tag{7.26}$$

In Eqs (7.11), (7.13), (7.19), (7.20) $\boldsymbol{u}$ is to be replaced by $[\![\boldsymbol{u}]\!]$ whilst in Eq (7.18) u_n, $\boldsymbol{u}_T$ by $[\![u_n]\!]$, $[\![\boldsymbol{u}_T]\!]$, respectively. The friction law takes the form

$$\boldsymbol{R}_T \in \partial_2(R_n, [\![\dot{\boldsymbol{u}}_T]\!]) \tag{7.27}$$

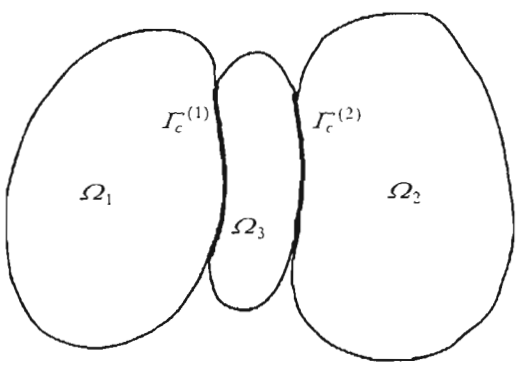

Fig. 4. Three contacting bodies

(vi) The contact bone-cement-prosthesis involves three bodies with two interfaces. To model such a system one has to consider the situation presented in Fig.4. On the interfaces Γ_c^α $(\alpha = 1, 2)$ the contact conditions can be similar or different. It seems, however, that the contact with adhesion between bone and the cement mantle should be modelled by somewhat different constitutive relationships than those describing the contact between two inorganic materials like cement and prosthesis. We hope to study this intriguing problem in the future.

7.3. Formulation of the initial-boundary value problem with adhesion

Let us consider the situation depicted in Fig.3. Both solids are assumed to be made of linear elastic, anisotropic and nonhomogeneous materials.

The system of equations (7.4) and (7.5) is to be replaced by

$$\begin{aligned} &\sigma_{ij,j}^{(\alpha)} + f_i^{(\alpha)} = 0 && \text{in } \Omega_{(\alpha)} \\ &\boldsymbol{u}^{(\alpha)} = \boldsymbol{0} && \text{on } \Gamma_0^{(\alpha)} \\ &\sigma_{ij}^{(\alpha)} n_j^{(\alpha)} = g_i^{(\alpha)} && \text{on } \Gamma_1^{(\alpha)} \\ &\sigma_{ij}^{(1)} n_j^{(1)} = -\sigma_{ij}^{(2)} n_j^{(2)} = R_i && \text{on } \Gamma_c \end{aligned} \tag{7.28}$$

and

$$\sigma_{ij}^{(\alpha)} = a_{ijkl}^{(\alpha)} e_{ij}(\boldsymbol{u}^{(\alpha)}) \tag{7.29}$$

where $\alpha = 1, 2$. All the quantities appearing in Eqs (7.28) and (7.29) depend on spatial variables and time $t \in [0, T]$. Here and below there is no summation over α. The initial conditions are specified by

$$\begin{aligned} &\beta(0, \boldsymbol{x}) = \beta_0(\boldsymbol{x}) && \boldsymbol{x} \in \Gamma_c \\ &\boldsymbol{u}^{(\alpha)}(0, \boldsymbol{x}^{(\alpha)}) = \boldsymbol{u}_0^{(\alpha)}(\boldsymbol{x}^{(\alpha)}) && \boldsymbol{x}^{(\alpha)} \in \Omega_{(\alpha)} \end{aligned} \tag{7.30}$$

We assume that adhesion is modelled by the functional (7.16) and

$$\varphi(\beta, [\![\boldsymbol{u}]\!]) = -\int_{\Gamma_c} w\beta \, d\Gamma + I_{K_1}(\beta, [\![\boldsymbol{u}]\!]) \tag{7.31}$$

where K_1 is defined by Eq (7.26). The presence of the indicator function I_{K_1} makes the functional φ non-differentiable. Having in mind approximate solutions we regularize it as follows, cf Point (1988)

$$\varphi_\varepsilon(\beta, [\![\boldsymbol{u}]\!]) = -\int_{\Gamma_c} w\beta \, d\Gamma + \frac{1}{4\varepsilon} \int_{\Gamma_c} \left[2\beta^2 \left| [\![\boldsymbol{u}]\!] \right|^2 + \left| (\beta - 1)^+ \right|^4 + \left| \beta^- \right|^4 + 2 \left| [\![\boldsymbol{u}_n]\!]^+ \right|^2 \right] d\Gamma \tag{7.32}$$

where $\varepsilon > 0$ and a^+ stands for the positive part of a whilst a^- for the negative part; similarly $[\![\boldsymbol{u}_n]\!]^+ = [\![u_n]\!]^+ \boldsymbol{n}$.

We set (the elastic moduli do not depend on t)

$$\begin{aligned} a^{(\alpha)}(\boldsymbol{u}^{(\alpha)}, \boldsymbol{v}^{(\alpha)}) &= \int_{\Omega_\alpha} a_{ijkl}^{(\alpha)}(\boldsymbol{x}) e_{ij}(\boldsymbol{u}^{(\alpha)}) e_{kl}(\boldsymbol{v}^{(\alpha)}) \, d\Omega_\alpha \\ l^{(\alpha)}(\boldsymbol{v}^{(\alpha)}) &= \int_{\Omega_\alpha} f_i^{(\alpha)} v_i^{(\alpha)} \, d\Omega_\alpha + \int_{\Gamma_1^\alpha} g_i^{(\alpha)} v_i^{(\alpha)} \, d\Gamma \end{aligned} \tag{7.33}$$

The approximate problem reads: find $\boldsymbol{u}^{(\alpha)}$ $(\alpha = 1, 2)$ vanishing on $\Gamma_0^{(\alpha)}$ and β such that

$$a^{(1)}(\boldsymbol{u}^{(1)}, \boldsymbol{v}^{(1)}) + a^{(2)}(\boldsymbol{u}^{(2)}, \boldsymbol{v}^{(2)}) + \frac{1}{\varepsilon}\int_{\Gamma_c}\left(\beta^2[\![\boldsymbol{u}]\!] + [\![\boldsymbol{u}_n]\!]^+\right)\cdot[\![\boldsymbol{v}]\!]\,d\Gamma = \tag{7.34}$$

$$= l^{(1)}(\boldsymbol{v}^{(1)}) + l^{(2)}(\boldsymbol{v}^{(2)})$$

for each $\boldsymbol{v}^{(\alpha)}$ vanishing on $\Gamma_0^{(\alpha)}$, and

$$\left(\langle\omega * \dot\beta, \dot\beta\rangle\right)^{\frac{p}{2}-1}\omega * \dot\beta = w - \frac{1}{\varepsilon}\left(\beta\left|[\![\boldsymbol{u}]\!]\right|^2 + \left|(\beta-1)^+\right|^3 - \left|\beta^-\right|^3\right) \quad \text{on } \Gamma_c \tag{7.35}$$

$$\beta(0, \boldsymbol{x}) = \beta_0(\boldsymbol{x}) \qquad \text{on } \Gamma_c$$

$$\boldsymbol{u}^{(\alpha)}(0, \boldsymbol{x}) = \boldsymbol{u}_0^{(\alpha)}(\boldsymbol{x}) \qquad \boldsymbol{x} \in \Omega_\alpha$$

Obviously, both β and $\boldsymbol{u}^{(\alpha)}$ depend on ε. We observe that the quantity

$$-\left(\frac{1}{\varepsilon}\beta^2[\![\boldsymbol{u}]\!] + \frac{1}{\varepsilon}[\![\boldsymbol{u}_n]\!]^+\right)$$

is an approximation of $\boldsymbol{R}$ whilst

$$-\left[w - \frac{1}{\varepsilon}\left(\beta\left|[\![\boldsymbol{u}]\!]\right|^2 + \left|(\beta-1)^+\right|^3 - \left|\beta^-\right|^3\right)\right]$$

is an approximation of F^i. It is also wort noting that precise formulation of the exact problem involves the notion of hemivariational inequality, which here we want to avoid.

Remark 7.1. To solve approximately adhesion problem with friction one has to regularize the functional of the total friction dissipation defined by

$$J(R_n, [\![\dot{\boldsymbol{u}}_T]\!]) = \int_{\Gamma_c} D(R_n, [\![\dot{\boldsymbol{u}}_T]\!])\,d\Gamma$$

This fact is well known in the numerical study of contact problems with friction, cf Telega (1988).

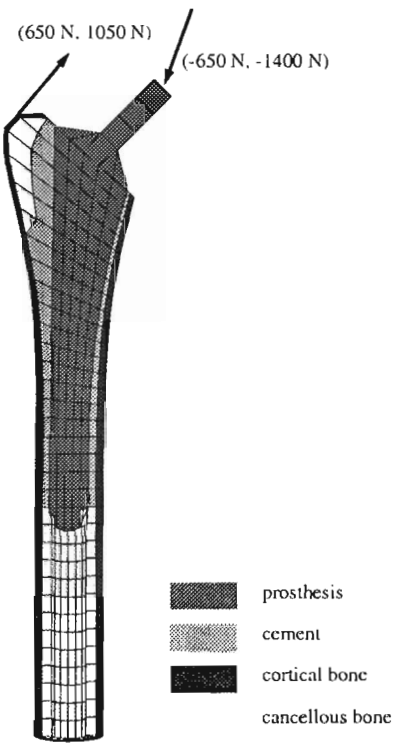

Fig. 5. Finite element model and loading conditions

8. Numerical example

8.1. Finite element model

Hip-prosthesis fixation have been studied using the developed contact algorithm with adhesion. We use a geometrically simplified three-dimensional finite element model of a femur with cemented implant shown in Fig.5. Considering loading in frontal plane we have assumed further the symmetry of the geometry with respect to the frontal plane. Reducing the size of the model by half we have treated realistically all other aspects of the modelling, so the model satisfies all the requirements to validate the developed contact algorithm.

589 eight-node isoparametric hexahedral elements were used in the discretization. Four materials: cortical bone, cancellous bone, cement and metal, have been considered in the model. The material parameters have been assumed

according to literature (Vichnin and Batterman, 1985). The stem was assumed to be of cobalt chromium alloy with the Young modulus $E = 214\,\text{GPa}$ and the Poisson ratio $\nu = 0.3$. The elastic modulus of the surgical cement was 2.27 GPa, and the Poisson ratio 0.335. Isotropic properties were also used for cancellous bone ($E = 0.325\,\text{GPa}$, $\nu = 0.29$) and for the cortical bone in the trochanteric region ($E = 11.5\,\text{GPa}$, $\nu = 0.32$). Transverse anisotropy was assumed for the cortical bone in the diaphysis with the moduli of elasticity $E_1 = 17\,\text{GPa}$ in the longitudinal direction, and $E_2 = E_3 = 11.5\,\text{GPa}$ in the transverse (radial and circumferential) directions. The material properties for transversal anisotropy are completed with the shear modulus in the longitudinal-transverse plane $G_1 = 3.28\,\text{GPa}$, and the Poisson ratios in the longitudinal-transverse plane $\nu_1 = 0.32$ and in the transverse-transverse plane $\nu_2 = 0.32$. All the material properties have been assumed homogenous.

Our model requires mechanical characteristics of the stem-cement and cement-bone interfaces. Following Mann et al. (1995) we have assumed the elastic modulus for the normal direction $E_n = 2200\,\text{MPa}$ and the shear modulus $G_s = 1100\,\text{MPa}$. The moduli E_n and G_n play the role of penalty coefficients for normal and tangential contact forces, respectively. The same values we have assumed for the cement-bone interface.

8.2. Loading conditions

The finite element model was fixed distally at the base of the bone and concentrated loads were applied to the prosthesis head and greater trochanter. The loading conditions approximated a one-legged stance. During the stance phase of walking, the hip joint force reaches its peak value (Bergmann et al., 1993). A strenuous loading was assumed corresponding to the peak force observed in fast walking at 6 km/h. The maximal value R_{max} of the resultant force observed (Bergmann et al., 1993) was 450% BW (body weight). Assuming the $\text{BW} = 700\,\text{N}$ we have $R_{max} = 3150\,\text{N}$. In reality the loading is not proportional, i.e., its direction changes in time. In our model we have assumed a proportional loading and neglected the component normal to the frontal plane (its peak value is about 10% of the resultant force). The two components of the hip joint force were taken according to the measurements of Bergmann et al. (1993) as 185% BW (1300 N) and 400% BW (2800 N) in the medial and distal directions, respectively. Since we analyzed half a structure only half of the above loading was applied (Fig.5).

The action of the main muscles of the thigh is simulated by the abducting force applied tangent to the greater trochanter (Fig.5). The abducting force was evaluated from the equilibrium condition at the hip joint. The joint

resultant force is the vectorial sum of the body weight and the muscle force (Cristofolini et al., 1995). Thus the lateral and proximal components of the abducting force employed in our model were 650 N and 1050 N, respectively (Fig.5). In order to avoid unrealistic stress concentrations the abducting force was distributed over the nodes in the trochanter.

8.3. Method of analysis

Behaviour of the femur with implant has been studied under quasi-static loading. The quasi-static loading, however, has been simulated using a dynamic explicit finite element program Stampack (Rojek et al., 1994, 1996).

The explicit dynamic method is based on the solution of the discretized equations of motion written in the following form in the current configuration

$$\mathbf{M}\ddot{\boldsymbol{a}} + \mathbf{C}\dot{\boldsymbol{a}} = \boldsymbol{p} - \boldsymbol{f} \tag{8.1}$$

where $\mathbf{M}$ and $\mathbf{C}$ are the mass and damping matrices, $\ddot{\boldsymbol{a}}$ and $\dot{\boldsymbol{a}}$ are the vectors of the nodal accelerations and velocities, $\boldsymbol{p}$ and $\boldsymbol{f}$ are the vectors of external loads and internal forces, respectively. The element internal force vector is calculated from the following relation

$$\boldsymbol{f}^{(e)} = \int_{V^{(e)}} \mathbf{B}^{\top}\boldsymbol{\sigma}\, dV \tag{8.2}$$

where $\boldsymbol{\sigma}$ is the Cauchy stress tensor, $\mathbf{B}$ is the strain-displacement operator matrix and $V^{(e)}$ is the element volume. The matrix $\mathbf{B}$ coincides with the standard form for infinitesimal geometrical changes if an updated Lagrangian formulation is used.

Eq (8.1) is integrated in time using an explicit scheme, in which the displacements $\boldsymbol{a}_{n+1}$ at time t_{n+1} are obtained from the equations for the known configuration at time t_n

$$\begin{aligned} \ddot{\boldsymbol{a}}_n &= \mathbf{M}_D^{-1}(\boldsymbol{p}_n - \boldsymbol{f}_n - \mathbf{C}\dot{\boldsymbol{a}}_n) \\ \dot{\boldsymbol{a}}_{n+\frac{1}{2}} &= \dot{\boldsymbol{a}}_{n-\frac{1}{2}} + \ddot{\boldsymbol{a}}_n \Delta t_{n+\frac{1}{2}} \\ \boldsymbol{a}_{n+1} &= \boldsymbol{a}_n + \dot{\boldsymbol{a}}_{n+\frac{1}{2}} \Delta t_{n+1} \end{aligned} \tag{8.3}$$

where

$$\mathbf{M}_D = \mathrm{diag}\mathbf{M} \qquad \Delta t_{n+\frac{1}{2}} = \frac{1}{2}(\Delta t_n + \Delta t_{n+1})$$

Now the subscript n denotes that a variable is taken at instant t_n. The effectiveness of the explicit dynamic formulation is based on the use of a diagonal mass matrix $\mathbf{M}_D$, so there is no need to solve a system of equations. The main disadvantage is the limitation of the time step size Δt due to the conditional stability of the integration scheme. Because of its efficiency in the analysis of large-scale systems the dynamic explicit approach has become very popular in many applications.

The dynamic analysis can also be used to analyse quasi-static problems. A structural response has a quasi-static character provided that:

- loading is introduced slowly during an interval sufficiently larger than the period of free vibrations,
- dynamic effects are damped out with structural damping.

Satisfying these requirements in the dynamic analysis we can obtain a quasi-static solution.

The first step of our analysis was the simulation of the dynamic problem without damping. The femur has been subjected to step-wise loading resulting in the response that allowed us to estimate the period of free vibrations in the lowest structural mode, $T_0 \approx 0.01\,\mathrm{s}$.

With the damping proportional to the mass matrix, i.e. $\mathbf{C} = 2\xi\mathbf{M}$, we estimate the critical damping $\mathbf{C}_{cr}$ for the lowest natural frequency ω_0 of the system as

$$\mathbf{C}_{cr} = \xi_{cr}\mathbf{M} \tag{8.4}$$

where

$$\xi_{cr} = \omega_0 = \frac{2\pi}{T_0}$$

8.4. Discussion of the results

With the damping evaluated as described above and increasing the load linearly in the interval of 0.02 s we have obtained a solution that can be regarded as quasi-static. This was controlled observing a displacement response of the loaded nodes. The final deformed shape of the femur with the implant is shown in Fig.6 compared with the initial configuration.

Fig.7 and Fig.8 show the distribution of the Huber-Mises and longitudinal stresses in the cortical bone. The medial surface of the cortical bone is in a compressive state, whereas the lateral surface is in a tensile one (Fig.8). The highest Huber-Mises stresses are observed near the end of the stem (Fig.7). The maximum compressive stresses on the medial surface are 35 MPa and

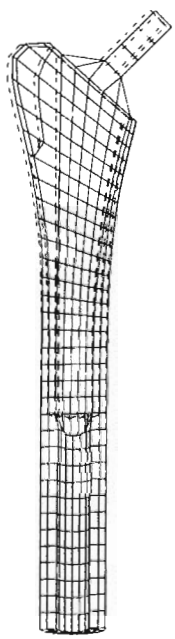

Fig. 6. Initial and deformed finite element mesh

the tensile stresses on the lateral surface near the end of the stem approach 21 MPa.

The aim of our study was to verify the new formulation of the contact algorithm with adhesion. In the studied problem the contact algorithm allowed both compressive and tensile pressure, the latter due to adhesion. Normal and shear contact stresses in the cement-stem interface are presented in Fig.9 and Fig.10, respectively. As it can be seen in Fig.10 on the end of the stem on the medial side we have high tensile stresses in the interface. The tensile stresses reaching about 12 MPa could cause debonding between the stem and cement. High shear stresses were also predicted at the end of the stem (Fig.9). The difference between our model considering adhesion and other models reported in literature consists in the possibility of taking into account shear stresses in the region with tensile normal streses until debonding is initiated. Our analysis, due to its incremental character, could detect initiation of debonding and development of debonding as the applied load is increased. Of course we consider here debonding due to high stresses not taking into account other possible reasons.

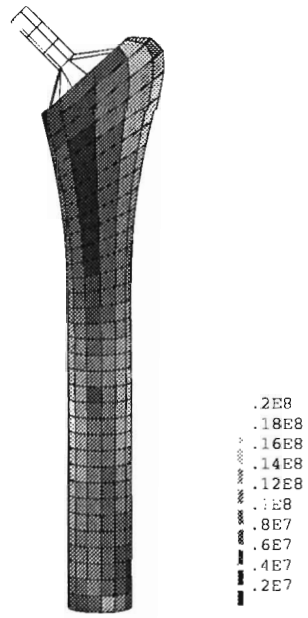

Fig. 7. Huber-Mises stresses in the cortical bone

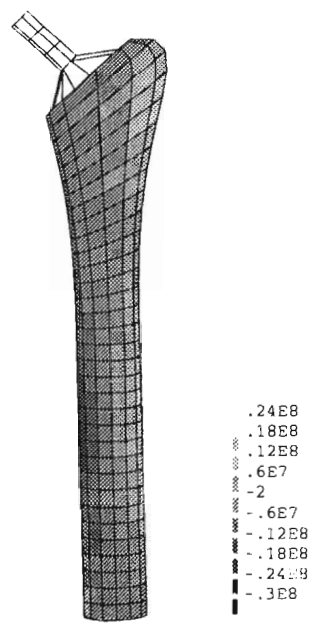

Fig. 8. Longitudinal stresses in the cortical bone

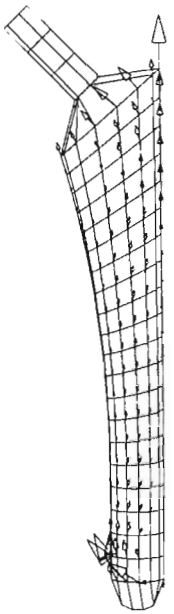

Fig. 9. Vectors of shear stresses in the stem-cement interface

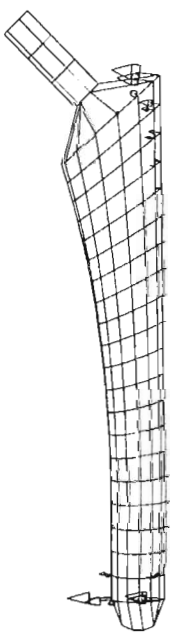

Fig. 10. Vectors of normal stresses in the stem-cement interface

9. Concluding remarks

Adhesion in the interfaces plays an important role in the fixation of prostheses. The developed algorithm of contact with adhesion allows us to obtain more realistic model of a bone-implant system than models with bonded interfaces or those using frictional contact without adhesion. Numerical analysis shows that loosening can be initiated by high tensile or shear stresses at the stem-cement interface. The formulation of the contact with adhesion allows us to consider not only tensile stresses at the interface but also the shear stresses in regions where there is still bonding and the contact pressure is non-compressive.

Acknowledgment

The works was supported by the State Committee for Scientific Research (KBN) through grant No. 8T11F01812.

References

1. BERGMANN G., GRAICHEN F., ROHLMANN A., 1993, Hip Joint Loading During Walking and Running, Measured in Two Patients, *J. Biomechanics*, **26**, 969-990

2. BOBYN J.D., PILLIAR R.M., BINNINGTON A.G., SZIVEK J.A., 1985, The Effect of Partially and Fully Porous Coated Hip Stem Design on Biological Fixation and Adaptive Bone Modelling, *Trans. Orthop. Res. Soc.*, 170

3. CRISTOFOLINI L., VICECONTI M., TONI A., GIUNTI A., 1995, Influence of Thigh Muscles on the Axial Strains in a Proximal Femur During Early Stance in Gait, *J. Biomechanics*, **28**, 617-624

4. CROWNINSHIELD R.D., BRAND R.A., JOHNSTON R.C., MILROY J.C., 1980, An Analysis of Femoral Component Stem Design in Total Hip Arthroplasty, *J. Bone Joint Surg.*, **62A**, 68-78

5. EVANS E., 1995, Physical Actions in Biological Adhesion, In R. Lipowsky and E. Sackmann, edit., *Handbook of Biological Physics*, 723-753, Elsevier Science

6. EVANS E., RITCHIE K., 1997, Dynamic Strength of Molecular Adhesion Bonds, *Biophysical J.*, **72**, 1541-1555

7. FREMOND M., 1987a, Adhérence des solides, *J. Méc. Théorique Appl.*, **6**, 383-407

8. FREMOND M., 1987b, Contact unilatéral avec adhérence: une théorie du premier gradient, In G. Del Piero and F. Maceri, edit., *Unilateral Problems in Structural Mechanics*, **2**, 117-197, Springer-Verlag, Wien-New York

9. FREMOND M., 1988, Contact with Adhesion, In J.J. Moreau and P.D. Panagiotopoulos, edit., *Nonsmooth Mechanics and Applications*, 177-221, Springer-Verlag, Wien

10. HARRIS W.H., 1992, Is It Advantageous to Strengthen the Cement-Metal Interface and Use a Collar for Cemented Femoral Components of Total Hip Replacements? *Clin. Orthop.*, **285**, 67-72

11. HUISKES R., 1979, Some Fundamental Aspects of Human Joint Replacements, *Acta Orthop. Scand.*, **185**, 1-208

12. HUISKES R., CHAO E.Y.S., 1983, A Survey of Finite Element Analysis in Orthopaedic Biomechanics: the First Decade, *J. Biomechanics*, **16**, 385-409

13. HUISKES R., JANSSEN J.D., SLOOFF T.J., 1982, Finite Element Analysis for Artificial Joint Fixation Problems in Orthopaedics, In R.H. Gallagher, B.R. Simon, P.C. Johnson, J.F. Gross, edit., *Finite Element in Biomechanics*, 313-342, Wiley

14. HUISKES R., VERDONSCHOT N., 1997, Biomechanics of Artificial Joints: the Hip, In V.C. Mow and W.C. Hayes, edit., *Basic Orthopaedic Biomechanics*, 395-460, Lippincott-Raven Publishers, Philadelphia

15. INGHAM E., FISCHER J., 1999, Wear of Ultra High Molecular Weight Polyethylene in Total Hip Joints, *Biological and Mechanical Mechanisms*, in press

16. KENDALL K., 1994, Adhesion: Molecules and Mechanics, *Science*, **264**, 1720-1725

17. KENDALL K., LIANG W., STAINTON C., 1998, New Theory and Observations of Cell Adhesion, *Proc. R. Soc. London*, **454**, 2529-2533

18. KRAUSE W.R., KRUG W., MILLER J., 1981, Strength of the Cement-Bone Interface, *Clin. Orthop.*, **163**, 290-299

19. MACKERLE J., 1998, A Finite Element Bibliography for Biomechanics, *Appl. Mech. Rev.*, **51**, 10, 587-634

20. MANN K.A., BARTEL D.L., WRIGHT T.M., BURSTEIN A.H., 1995, Coulomb Frictional Interfaces in Modelling Cemented Total Hip Replacement: a More Realistic Model, *J. Biomechanics*, **28**, 1067-1078

21. MAUGIS D., 1982, Adherence of Solids, In J.M. Georges, edit., *Microscopic Aspects of Adhesion and Lubrication*, 221-252, Elsevier, Amsterdam

22. MAUGIS D., BARQUINS M., 1980, Fracture Mechanics and Adherence of Viscoplastic Solids, In H.-L. Lee, edit., *Adhesion and Adsorption of Polymers*, Part A, 203-277, Plenum Publishing Corporation, New York

23. MCNAMARA B.P., CRISTOFOLINI L., TONI A., TAYLOR D., 1997, Relationship Between Bone-Prosthesis Bonding and Load Transfer in Total Hip Reconstruction, *J. Biomechanics*, **30**, 621-630

24. MOREAU J.J., 1988, Bounded Variation in Time, In J.J. Moreau, P.D. Panagiotopoulos, and G. Strang, edit., *Topics in Nonsmooth Mechanics*, 1-74, Birkhauser Verlag, Basel

25. POINT N., 1988, Unilateral Contact with Adherence, *Math. Meth. Appl. Sci.*, **10**, 367-381

26. RAAB S., AHMED A.M., PROVAN J.W., 1981, The Quasistatic and Fatigue Performance of the Implant/Bone-Cement Interface, *J. Biomed. Mat. Res.*, **15**, 159-182

27. RAUT V.V., KAY P., SINEY P.D., WROBLEWSKI B.M., 1997, Factors Affecting Socket Fixation after Cemented Revision, *Int. Orthoapeadics (SICOT)*, **21**, 83-86

28. ROCKFELLAR R.T., WETS R.J.-B., 1998, *Variational Analysis*, Springer, Berlin

29. ROHLMANN A., CHEAL E.J., HAYES W.C., BERGMANN G., 1988, A Nonlinear Finite Element Analysis of Interface Conditions in Porous Coated Hip Endoprostheses, *J. Biomechanics*, **21**, 605-611

30. ROJEK J., HERRE J., OÑATE E., 1994, *STAMPACK: an Explicit Finite Element Program for Analysis of Sheet Stamping Problems*, Technical Report No. IT-159, CIMNE, Barcelona

31. ROJEK J., JOVICEVIC J., OÑATE E., 1996, Industrial Applications of Sheet Stamping Simulation Using New Finite Element Models, *Journal of Materials Processing Technology*, **60**, 243-247

32. RUBIN P.J., RAKOTOMANANA R.L., LEYVRAZ P.F., ZYSSET P.K., CURNIER A., HEEGAARD J.H., 1992, Frictional Interface Micromotions and Anisotropic Stress Distribution in a Femoral Total Hip Component, *J. Biomechanics*, **26**, 725-739

33. TELEGA J.J., 1988, Topics of Unilateral Contact Problems of Elasticity and Inelasticity, In J.J. Moreau and P.D. Panagiotopoulos, edit., *Nonsmooth Mechanics and Applications*, 341-462, Springer-Verlag, Wien-New York

34. TELEGA J.J., GAŁKA A., 1998, Dynamic Contact Problems for Systems with Finite Degrees of Freedom: the Case of Piecewise Regular Constraints, *Math. Comput. Modelling*, **28**, 479-495

35. TELEGA J.J., GAŁKA A., KOWALCZEWSKI J., MAŁDYK P., 1999, Friction and Wear in Natural and Artificial Joints, *Eng. Trans.*

36. VICHNIN H.H., BATTERMAN S.C., 1985, Stress Analysis and Failure Prediction in the Proximal Femur Before and After Total Hip Replacement, *J. Biomech. Eng.*, **108**, 33-41

37. WALKER P.S., BLUNN G.W., 1997, Biomechanical Principles of Total Knee Replacement Design, In V.C. Mow and W.C. Hayes, editors, *Basic Orthopaedic Biomechanics*, 461-493, Lippincott-Raven Publishers, Philadelphia

38. WEINANS H., HUISKES R., GROOTENBOER H.J., 1990, Trends of Mechanical Consequences and Modeling of a Fibrous Membrane Around Femoral Hip Prostheses, *J. Biomechanics*, **23**, 991-1000

39. WILLERT H.G., LUDWIG J., SEMLITSCH M., 1974, Reaction of Bone to Methacrylate after Hip Arthroplasty, *J. Bone Joint Surg.*, **56-A**, 1368-1382

Numeryczna symulacja układów kość-implant z uwzględnieniem bardziej realistycznego kontaktu z adhezją

Streszczenie

Cel pracy jest dwojaki. Po pierwsze, zostały przedyskutowane najważniejsze pojęcia dotyczące adhezji. Zbadano zagadnienie modelowania jednostronnego kontaku z adhezją pomiędzy dwoma odkształcalnymi ciałami. Sformułowano kontaktowe zadanie początkowo-brzegowe z adhezją i przeprowadzono jego regularyzację. Po drugie, przeprowadzono analizę numeryczną zachowania się kości biodrowej z implantem w przypadku obciążenia kwasi-statycznego.

Manuscript received January 14, 1999; accepted for print March 3, 1999